Ecological Modelling 222 (2011) 76–90

Contents lists available at ScienceDirect

Ecological Modelling

journal homepage: www.elsevier.com/locate/ecolmodel

Modeling the impacts of calcite precipitation on the epilimnion of an ultraoligotrophic, hard-water lake

Elizabeth S. Homa*, Steven C. Chapra[1]

Civil and Environmental Engineering Department, Tufts University, 223 Anderson Hall, Medford, MA 02155, USA

ARTICLE INFO

Article history:
Received 18 May 2010
Received in revised form 30 August 2010
Accepted 8 September 2010
Available online 11 October 2010

Keywords:
Calcite precipitation
Calcium carbonate
Alkalinity
Turbidity
Water quality model
Light extinction

ABSTRACT

A mass-balance model of calcite precipitation was developed to investigate the interactions of the varied processes governing the generation and fate of calcite in lakes. The model was used in conjunction with data to assess the evolution and impact of calcite precipitation for calcareous, ultraoligotrophic Torch Lake, Michigan (USA). This lake is an ideal setting for implementation of a baseline modeling study of calcite precipitation where the physical drivers could be evaluated without being dominated, as in many systems, by biological processes. The model provides a representation of calcite precipitation with particulate surface area changing over time, and demonstrates that it is possible for the change in water clarity to be explained by calcite precipitation employing standard optical models. Using the mass balance model to quantify the roles of the various chemical, biological and physical processes interacting in the lake's epilimnion, it was shown that the seasonal temperature rise and air–water CO_2 exchange drive calcite precipitation much more than primary production for this ultraoligotrophic system.

1. Introduction

Calcite precipitation is a prominent phenomenon in hard-water lakes that can occur when the product of the calcium and carbonate ion activities exceeds calcite's solubility product. Such oversaturation depends on multiple factors. First, from a strictly physicochemical perspective, rising epilimnetic temperatures contribute to oversaturation by decreasing calcite's solubility product while shifting the inorganic carbon equilibrium towards carbonate (Plummer and Busenberg, 1982; Stumm and Morgan, 1996). Second, in productive systems, photosynthetic carbon-dioxide uptake raises the pH with an attendant shift of inorganic carbon speciation towards carbonate (Hodell et al., 1998; Ramisch et al., 1999).

Whereas oversaturation is a prerequisite for precipitation, a high level of oversaturation of calcite is often observed in natural waters before precipitation actually occurs (Morel and Hering, 1993; Hodell et al., 1998). However, the actual level of oversaturation required is greatly reduced by the presence of seed particles. For example, picoplankton (plankton ranging in size from 0.5 to 2 μm) have been identified as providing ideal surfaces for calcite nucleation in oligotrophic lakes. Beyond providing nucleation sites, picoplankton may also enhance precipitation by creating a favorable microenvironment which may provide increased local saturation levels and other surface characteristics supporting nucleation (Thompson et al., 1997; Dittrich and Obst, 2004; Dittrich et al., 2004).

Once formed, the calcite crystals influence physical, chemical and biological processes in a variety of ways. Because of their size and optical properties, calcite crystals settle slowly and scatter light very efficiently. As a consequence, they remain in suspension with a significant reduction in water clarity. The phenomenon is commonly called a "whiting" due to the characteristic milky-white color imparted to the water by the calcite crystals (Kalff, 2003). The associated reduction in light penetration has both biological (photosynthesis) and physical (heat penetration and thermal stratification) effects. In addition, the decrease in water clarity can have a negative influence on human perception of the lake's quality and economic value related to aesthetics and recreation.

Beyond water clarity and light transmission, calcite precipitation serves as a chemical safety valve that moderates pH rises by removing carbonate. It is also known that both inorganic nutrients such as phosphorus as well as dissolved organic compounds can attach to calcite particles (Kleiner, 1988; House, 1990; Danenlouwerse et al., 1995). In the short-term, this reduces the availability of these compounds for biological utilization. If the settling particles do not subsequently dissolve and are permanently buried in the lake's bottom sediments, the process can enhance the long-term removal of calcium and inorganic carbon, as well as nutrients and organics (Dittrich and Koschel, 2002).

* Corresponding author. Tel.: +1 781 235 5576; fax: +1 617 627 3994.
E-mail addresses: homa@post.harvard.edu (E.S. Homa), steven.chapra@tufts.edu (S.C. Chapra).
[1] Tel.: +1 617 627 3654.

0304-3800/$ – see front matter © 2010 Elsevier B.V. All rights reserved.
doi:10.1016/j.ecolmodel.2010.09.011

Nomenclature

a	absorption coefficient, m^{-1}
a_c	color absorption coefficient, m^{-1}
Alk	alkalinity, eq/L
Alk_{nc}	non-calcium alkalinity, eq/L
a_p	phytoplankton, μg Chla/L
A_s	lake surface area, m^2
A_t	thermocline area, m^2
a_w	water absorption coefficient, m^{-1}
b	scattering coefficient, m^{-1}
b_w	water scattering coefficient, m^{-1}
$SA_{v,a}$	phytoplankton volume-specific surface area, m^2
$SA_{v,c}$	calcite volume-specific surface area, m^2
c	beam attenuation coefficient, m^{-1}
$[Ca^{2+}]$	dissolved calcium concentration, M
$[CaCO_{3(s)}]$	calcite concentration, M
$[CO_2]$	carbon dioxide concentration, M
$[CO_2]_s$	saturation concentration of carbon dioxide, M
$[CO_3{}^{2-}]$	carbonate concentration, M
Cond	specific conductance, $\mu S\,cm^{-1}$
c_T	total inorganic carbon, M
E_g	a chemical enhancement factor dimensionless
f	photoperiod, d
F_d	fraction of inorganic phosphorus dissolved
F_p	fraction of inorganic phosphorus associated with calcite
H	average depth of epilimnion, m
$[H_2CO_3{}^*]$	sum of dissolved carbon dioxide and carbonic acid concentrations, M
$[HCO_3{}^-]$	bicarbonate ion concentration, M
$I(0)$	surface PAR, $\mu E/m^2/s$
ISS	non-calcite inorganic suspended solids, mgD/L
IAP	ion activity product
k_{de}	phytoplankton death rate, /d
K_{dp}	partition coefficient of inorganic phosphorus on calcite, M^{-1}
k_e	light extinction coefficient, /m
k_f	area-specific precipitation rate, $L/(M\,m^2\,d)$
k_g	phytoplankton growth rate, /d
K_H	Henry's constant, M/atm
k_{hy}	hydrolysis rate, /d
k_{re}	phytoplankton respiration/excretion rate, /d
K_{sp}	calcite solubility product, M^2
k_{si}	PAR half-saturation constant, $\mu E/m^2/s$
k_{sp}	dissolved inorganic phosphorus half-saturation constant, μg P/L
mM_i	millimolar concentration of ith ion, mM
N	ratio of NTU turbidity to scattering NTU, m
GPP	Gross primary productivity, $mg\,C/m^2/d$
PAR	photosynthetically active radiation, $\mu E/m^2/s$
p_{CO_2}	partial pressure of carbon dioxide in atmosphere, atm
pH	pH
p_i	inorganic phosphorus concentration, μg P/L
p_o	organic phosphorus concentration, μg P/L
NPP	net primary productivity, $mg\,C/m^2/d$
TP	total phosphorus concentration, μg P/L
Q	flow, m^3/d
r_{ca}	ratio of inorganic carbon to phytoplankton biomass, M/μg Chla
r_{coa}	ratio of phytoplankton organic carbon to chlorophyll a, mg C/μg Chla
r_{cp}	ratio of inorganic carbon to phosphorus, M/μg P
r_{da}	ratio of phytoplankton dry weight to chlorophyll a, mg D/μg Chla
r_{dc}	a conversion to convert moles of calcite to mass, $mg\,CaCO_3/M$
r_{pa}	ratio of phosphorus to chlorophyll, μg P/μg Chla
SA	total particulate surface area, m^2/L
S	kinetic interactions, mg/(L d)
Sc	Schmidt number for carbon dioxide
SD	Secchi depth, m
t	time, d
T	temperature, °C
T_a	absolute temperature, K
T_N	turbidity, NTU
V	epilimnion volume, m^3
v_a	phytoplankton settling velocity, m/d
v_c	calcite settling velocity, m/d
v_o	organic (detrital) phosphorus settling velocity, m/d
$v_{v,c}$	carbon-dioxide mass-transfer coefficient, m/d
z	depth, m
Z_i	charge of ith ion
H	thermocline thickness, m

Greek letters

φ	solar zenith angle at solar noon radians
θ	temperature-dependence parameter dimensionless
$\gamma(z)$	activity coefficient
α_{chl}	absorption proportionality constant for chlorophyll a, m^2/mg Chla
α_{op}	absorption proportionality constant for organic P, m^2/mg P
α_i	absorption proportionality constant for inorganic suspended solids, $m^2/g\,D$
$\beta_{calcite}$	scattering proportionality constant for calcite, 1/(mM)
β_{chl}	scattering proportionality constant for chlorophyll a, m^2/mg Chla
β_{op}	scattering proportionality constant for detritus, m^2/mg P
β_i	scattering proportionality constant for inorganic suspended solids, $m^2/g\,D$
λ_i	equivalent conductance of ith ion, mho cm^2/equiv.
ϕ_l	light limitation factor dimensionless
ϕ_p	phosphorus limitation factor dimensionless

Although the phenomenon has been well-studied scientifically, it has not been incorporated into water-quality modeling frameworks in a comprehensive fashion. In particular, no currently available modeling framework encompasses the phenomenon's multi-faceted nature by integrating nutrient/phytoplankton interactions (i.e., eutrophication), inorganic chemistry (i.e., calcite precipitation, inorganic carbon dynamics, and pH) and optics (i.e., light extinction and scattering).

The current study investigates the evolution of calcite precipitation for the epilimnion of an ultraoligotrophic, calcareous lake: Torch Lake (MI, USA). The lake which is noteworthy for its exceptional clarity (spring Secchi depths on the order of 12 m), was chosen because it routinely experiences dramatic reductions (more than 50%) in Secchi disk depth during the summer stratified period. Because it is so nutrient poor, the lake is particularly well-suited for assessing the impact of calcite precipitation on the water quality of a pristine, low-productivity lake.

An extensive data set consisting of physical and chemical measurements was collected during the summer of 2006. A dynamic

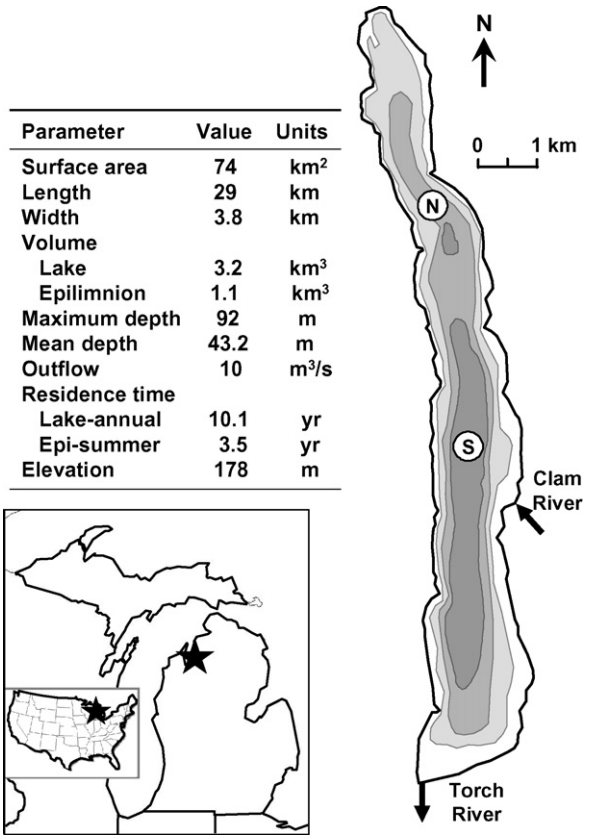

Fig. 1. Torch Lake, Michigan showing major inflow, outflow and primary deep-water sampling sites: North Basin (N) and South Basin (S). The insets indicate the lake's location and the table provides a summary of its physical characteristics.

mass-balance model of the lake's epilimnion is employed to synthesize these observations and investigate the interactions of the various processes that generate and remove calcite and other chemical constituents during summer stratification. Along with the biochemical budgets, a model of water transparency is also developed to link calcite precipitation to light extinction, turbidity, and Secchi disc depth. Multiple cross-checks and independent estimates are developed to calibrate and bound the model parameters.

The increase in pH due to CO_2 removal by primary production has often been proposed as the primary driver for calcite precipitation (Hodell et al., 1998; Ramisch et al., 1999). Given the ultraoligotrophic state of Torch Lake, the model was used to evaluate whether other processes were driving calcite precipitation in this system. Using the model to analyze the interactions of the basic biological, physical and chemical processes affecting the lake's carbon cycle, we assert that CO_2 loss to the air shifts the carbonate cycle towards precipitation much more than phytoplankton growth. Temperature also acts as a key driver by directly affecting the rate of calcite precipitation as well as influencing the rate of air–water exchange of carbon dioxide.

2. Materials and methods

2.1. Study site

Torch Lake (latitude: 45.98°; longitude: −85.30°) is located in the lower peninsula of Michigan to the east of Grand Traverse Bay (Fig. 1). The glacial lake is deep and elongated with an average residence time of about a decade. It is noted for its exceptional beauty due to its unusually clear and turquoise-hued waters. This quality has made the lake a popular and highly valued locale for resorts and vacation homes.

Table 1
Chemical, biological and optical characteristics of Torch Lake, MI. Values for) trophic state index (TSI) are also tabulated. Note that a TSI < 27.4 connotes ultraoligotrophic conditions based on) suggested criterion for ultraoligotrophy as total phosphorus concentration < 5 μg/L.

Parameter	Value	Units	TSI
Alkalinity	2.7	mequiv./L	
	135	mg $CaCO_3$/L	
Calcium	1	mM	
	40	mg/L	
Total phosphorus	0.08	mM	
	2.5	μg P/L	17.4
Summer chlorophyll *a*	0.5	μg Chla/L	23.8
Secchi depth			
Spring	12	m	24.2
Late summer	5	m	36.8

Table 2
Summary of major Torch Lake data collection efforts conducted by the Three Lakes Association (TLA); Michigan State University (MSU); the Great Lakes Environmental Center (GLEC); Tufts University (TU); the Michigan Water Research Center (MWRC); and the Upstate Freshwater Institute (UFI).

Type	Period	Organization
Secchi depths	1997–2008	TLA
Sediment cores	2002	MSU
Comprehensive lake, inflows, groundwater, sediments	2004–2005	TLA; GLEC
Lake water quality with focus on calcite and optics	2006	TLA; TU; MWRC; UFI

As summarized in Table 1, Torch Lake is ultraoligotrophic with very low levels of total phosphorus (2.5 μg P/L) and phytoplankton biomass (0.5 μg Chla/L). In addition, the lake is high in calcium (1 mM) and alkalinity (2.7 mequiv./L), both typical of lakes in the region and similar to neighboring Lake Michigan.

Although it is certainly ultraoligotrophic, with minimal nutrients and phytoplankton biomass, the lake experiences a consistent decrease in water clarity every summer. As depicted in Fig. 2, the Secchi disk decreases from about 12 to 5 m over the period from late May through August. One of the goals of this study was to confirm that this reduction in clarity could be explained overwhelmingly by calcite precipitation.

2.2. Data

As summarized in Table 2, a number of data collection efforts have been conducted on the Torch Lake system over the past decade. The Three Lakes Association (TLA) has routinely measured Secchi disk depth from 1997 through the present (Fig. 2). These

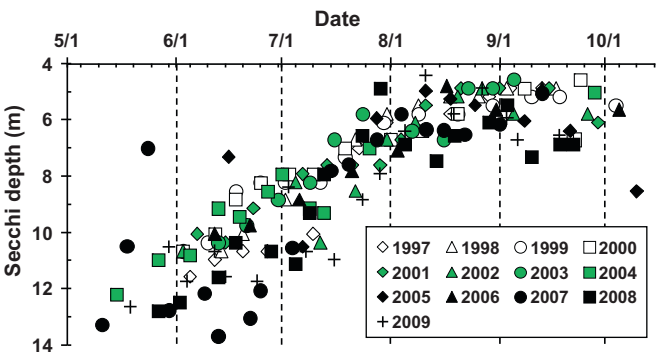

Fig. 2. Secchi disc depth (m) versus date for Torch Lake, Michigan for June to October 1997–2009.

measurements were typically taken at both the North and South basin deep-water stations (Fig. 1) on a weekly to bi-weekly frequency during the ice-free period. In most cases, the depth was measured by two different individuals and the average taken of these measurements.

Sediment cores were collected for Torch Lake in 2002 as part of a study conducted by Michigan State University of trends in the sediment quality of Michigan lakes (Yohn et al., 2003). This study yielded estimates of a sedimentation rate for Torch Lake of 447 g/m^2/yr, along with calcium (31.2% by mass) and phosphorus (0.035% by mass) content of the cores. These values were then used to calibrate the calcite settling velocity parameter and the coprecipitation rate in our model.

In 2004 and 2005, the TLA and the Great Lakes Environmental Center (GLEC) undertook a study that included comprehensive field data collection. From July of 2004 through October of 2005, physical/chemical (pH, dissolved oxygen, temperature, conductivity, total phosphorus) and biological (chlorophyll *a*) data were collected in the lake, and total phosphorus concentrations were also measured in tributaries, groundwater and lake sediments (Bretz et al., 2005; Endicott et al., 2006).

From June 8 to September 13, 2006, a comprehensive data collection effort was conducted with special emphasis on measurements related to calcite dynamics and optics. Water-quality samples were collected at the North Basin deep-water station on a bi-weekly basis. Temperature, pH, conductivity, and dissolved oxygen (DO) data were measured with a Hydrolab Quanta® every 3 m to a depth of 30 m, then every 10 m to the lake bottom. Volume-weighted averages were calculated from these measurements for the epilimnion and hypolimnion.

Grab samples were collected with a Van Dorn Sampler at three different depths (2, 6, and 10 m) and then composited as an epilimnion sample. The hydrolab temperature profiles show the depth of the top of the thermocline ranging from 10 to 17 m over the summer sampling period. We opted to have fixed sampling depths that were always within the mixed section of the epilimnion. The same was done at depths of 40, 50, and 60 m in order to accurately characterize the hypolimnion. Subsamples of each composite were used to measure turbidity, particulate calcium, dissolved calcium and alkalinity for both the epilimnion and hypolimnion. The turbidity of each composite was measured on board with a Hach 2100P Portable Turbidimeter.

A composite epilimnion sample of 500 mL was filtered on board through Gelman Nylaflo 0.45-μm, 47-mm filters. The filters were then sent to A&L Great Lakes Laboratories, where they were digested in nitric acid, diluted to approximately 25 mL and analyzed for mg/L calcium by ICP-MS. The amount of particulate calcium found on the filter in relation to the amount of lake water filtered was used to quantify the particulate calcite concentration. Subsamples were sent to the Michigan Water Research Center (Central Michigan University) for determination of dissolved calcium by EDTA titration and alkalinity by titration.

Photosynthetically active radiation (PAR) was measured every 3 m to a depth of 36 m or until 1% of the surface measurement was reached with a Licor LI193SA Spherical Quantum Sensor and LI250A Light Meter. Secchi disk was measured by two different individuals and the average taken of these measurements.

Van Dorn samples were taken at a 2-m depth and sent overnight in a foam un-iced cooler to the Upstate Freshwater Institute (UFI) where inorganic particles were morphometrically and elementally characterized by individual particle analysis conducted with scanning electron microscopy interfaced with automated image and X-ray analyses (IPA/SAX). Particle types were classified based on mineral composition and particle distribution data by number and volume were generated. The methods used are described in detail by Peng and Effler (2005).

Table 3
Model state variables.

Variable	Symbol	Units[a]
Nutrient/phytoplankton		
Phytoplankton	a_p	μg Chla/L
Organic phosphorus	p_o	μg P/L
Inorganic phosphorus	p_i	μg P/L
Inorganic chemistry		
Total inorganic carbon	c_T	M
Total dissolved calcium	$[Ca^{2+}]$	M
Calcite	$[CaCO_{3(s)}]$	M

[a] μg/L ≡ mg/m^3; and M ≡ mol/L. In addition, the terms Chla and P refer to chlorophyll *a* and phosphorus, respectively.

A four-inch diameter cylindrical sediment trap was set in the North Basin sampling location at a depth of 40 m on June 26 and retrieved on October 5, 2006. The contents were analyzed at GLEC for total dry mass (1.28 g), magnesium (0.01%) and calcium (42%).

2.3. Model development

The following model is expressly designed as a data synthesis tool, rather than as a comprehensive predictive framework. Consequently, we have taken a parsimonious approach by developing a model and collecting data to characterize the minimum set of processes required to provide an initial quantification of the role of calcite precipitation in the carbon cycle of this ultraoligotrophic lake. After a general overview, the following description emphasizes aspects of the model that are either novel or are specifically related to the focus of the current application.

2.3.1. Overview

The model state variables are those constituents for which mass balances are written and solved as a function of time (Table 3). Note that concentrations are expressed in a variety of units. In addition, both concentrations and activities are employed for equilibrium chemistry calculations. Different style brackets are used to distinguish between molar concentrations [ ] and activities { }. Activity corrections are made with the Davies equation (Davies, 1962; Allison et al., 1991).

As depicted in Fig. 3, the epilimnion is represented as a completely mixed, constant-volume system with differing top (air–water interface) and bottom (thermocline) areas. All state variables are transported via inflow, outflow, and thermocline diffusion. In addition, particulate forms settle across the thermocline and carbon dioxide is transferred across the air–water interface.

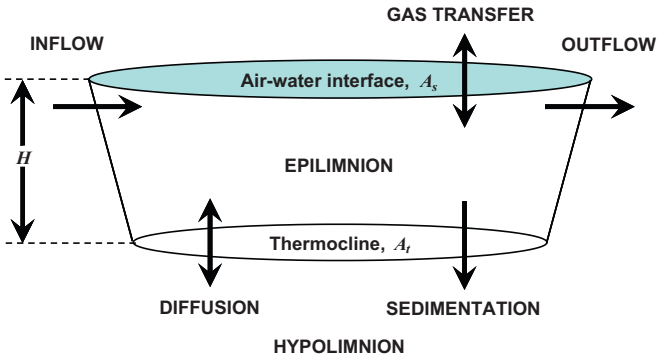

Fig. 3. The epilimnion of a lake showing model transport processes.

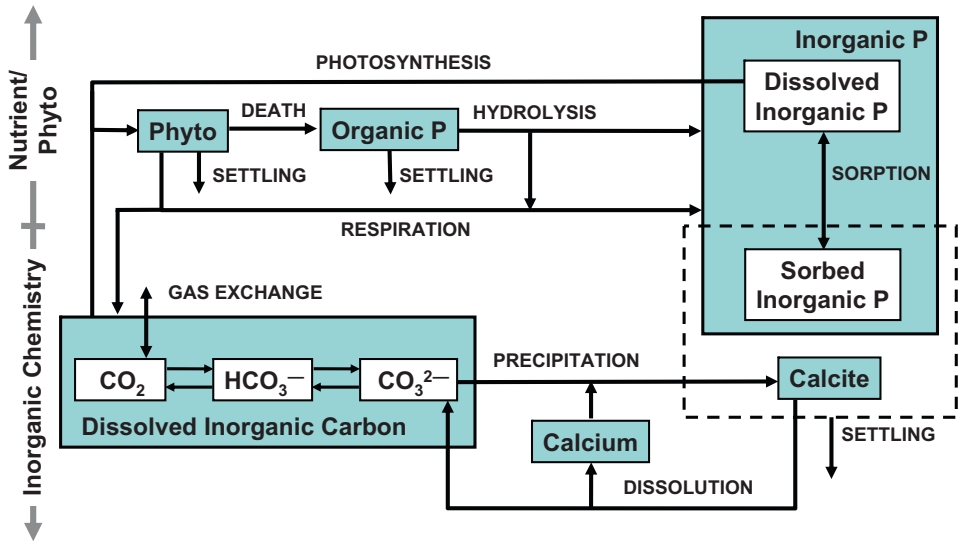

Fig. 4. Kinetic relationships among the model state variables.

Table 4
Kinetic interactions and stoichiometry. Nutrient/phytoplankton sub model processes above divider and state variables to the left. Inorganic chemistry sub model processes below divider and state variables to the right.

Component→ Process↓	a_p	p_o	p_i	c_T	$[Ca^{2+}]$	$[CaCO_{3(s)}]$	Process rates, (Mass/Volume)/Time
Nutrient/phytoplankton							
Photosynthesis	1		$-r_{pa}$	$-r_{ca}$			$k_g\,\phi_p\,\phi_l\,a_p$
Respiration/excretion	−1		r_{pa}	r_{ca}			$k_{re}\,a_p$
Hydrolysis		−1	1	r_{cp}			$k_{hy}\,p_o$
Death	−1	r_{pa}					$k_{de}\,a_p$
Phytoplankton settling	−1						$v_a\,(A_t/V)\,a_p$
Organic P settling		−1					$v_o\,(A_t/V)\,p_o$
Inorganic chemistry							
Calcite precipitation				−1	−1	1	$k_f\,SA\,([Ca^{2+}][CO_3{}^{2-}]-K_{sp})$
CO_2 air-water exchange				1			$E_g v_{v,c}(A_s/V)([CO_2]_s-[CO_2])$
Calcite settling			$-K_{dp}F_d p_i$			−1	$v_c\,(A_t/V)\,[CaCO_{3(s)}]$

A general mass balance for each state variable can be written for this layer as

$$\frac{dc}{dt} = \frac{Q_{in}}{V}c_{in} - \frac{Q_{out}}{V}c + \frac{E'_{12}}{V}(c_{hyp} - c) + S \quad (1)$$

where c = epilimnion concentration (μg/L ≡ mg/m³),[2] t = time (d), Q_{in} = inflow (m³/d), Q_{out} = outflow (m³/d), V = epilimnion volume (m³), c_{in} = inflow concentration (μg/L), E'_{12} = bulk thermocline diffusion coefficient (m³/d), c_{hyp} = hypolimnion concentration (μg/L), and S = kinetic interactions [μg/(L d)]. The bulk diffusion coefficient (Chapra, 1979) is a phenomenological parameter that quantifies mass transfer due to turbulent mixing across open boundaries (in this case, the thermocline).

As depicted in Fig. 4, two coupled sub-models are designed to simulate (1) nutrient cycling and phytoplankton dynamics and (2) inorganic chemistry equilibria and kinetics. In addition, an optics sub-model calculates both inherent and apparent optical properties as a function of output from the eutrophication and inorganic chemistry sub-models.

The underlying processes and associated stoichiometric conversions are summarized in Table 4. Organic matter is assumed to have constant stoichiometry following the Redfield ratio (Redfield et al., 1963). The stoichiometry of photosynthesis and respiration/excretion is represented by (Stumm and Morgan, 1996)

$$106CO_2 + 16NH_4^+ + HPO_4^{2-} + 106H_2O \underset{R}{\overset{P}{\rightleftharpoons}} C_{106}H_{263}O_{110}N_{16}P_1 + 106O_2 + 14H^+ \quad (2)$$

It is also assumed that the phosphorus-to-chlorophyll ratio in mass units is 1 μg P/μg Chla (Reynolds, 1984). Consequently, phytoplankton concentrations can be interpreted as either chlorophyll or phosphorus units.

Stoichiometric conversions in Table 4 are computed generally as $r_{xy} = M_x/M_y$ where M_x = mass of X and M_y = mass of Y. Other parameters shown in Table 4 are defined in the nomenclature section and described in the subsequent paragraphs. Note that an Arrhenius or "theta" model is used to represent the temperature effect for all first-order reactions,

$$k(T) = k(20)\theta^{T-20} \quad (3)$$

where $k(T)$ = the reaction rate [/d] at temperature T [°C] and θ = the temperature parameter for the reaction. For this model, the basic heuristic of a doubling of the rate with an increase of 10 °C was used for all reaction rates (θ = 1.072).

Given specified initial conditions, the mass-balance equations are integrated numerically to yield concentrations of the state variables as a function of time. At each time step, a number of secondary variables (Table 5) are computed based on the state variables. In addition to their employment in the process kinetics (e.g., light

[2] Although we use μg/L to generally represent concentration in Eq. (1), molar units are employed for the inorganic chemistry state variables as listed in Table 4.

Table 5
Model secondary variables.

Variable	Symbol	Units
Nutrient/phytoplankton		
Gross primary productivity	*GPP*	mg C/m^2/d
Net primary productivity	*NPP*	mg C/m^2/d
Total phosphorus	*TP*	μg P/L
Inorganic chemistry		
Alkalinity	*Alk*	eq/L
Specific conductance	Cond	μS cm^{-1}
Dissolved carbon dioxide	[CO_2]	M
Bicarbonate	[HCO_3^-]	M
Carbonate	[CO_3^{2-}]	M
pH	pH	
Optics		
Secchi depth	*SD*	m
Extinction coefficient	k_e	/m
Turbidity	T_N	NTU

extinction), these secondary variables also provide supplementary metrics for assessing model performance and behavior.

2.3.2. Nutrient/phytoplankton sub-model

Although biotic impacts on calcite formation should be minimal for this ultraoligotrophic system, we have included a simple nutrient/phytoplankton sub-model for completeness. This sub-model is designed to simulate phytoplankton/nutrient dynamics for a phosphorus-limited system. Although more detailed nutrient/food-chain frameworks are certainly available (e.g., Canale et al., 1975; Hamilton and Schladow, 1997; Arhonditsis and Brett, 2005, etc.), we propose that our parsimonious representation is appropriate for the Torch Lake system. For cases with higher productivity and more complete biological data sets, these more detailed frameworks could be readily integrated into our framework.

Three primary state variables are employed to characterize phytoplankton/nutrient interactions: phytoplankton biomass, organic phosphorus and inorganic phosphorus (Schnoor and O'Connor, 1980). Organic phosphorus corresponds to non-phytoplankton organic species (e.g., dissolved organic phosphorus, detrital phosphorus, etc.) that must be converted to the available inorganic form prior to phytoplankton uptake. Note that organic phosphorus also serves as a surrogate for non-phytoplankton organic carbon for use in the total inorganic carbon balance as well as in the optics sub-model.

Inorganic phosphorus represents the sum of (a) dissolved forms that can be readily taken up by phytoplankton (e.g., soluble reactive phosphorus) and (b) particulate inorganic phosphorus that is sorbed or "coprecipitated" onto calcite particles,

$$p_i = p_{i,d} + p_{i,p} \tag{4}$$

where $p_{i,d}$ = dissolved inorganic phosphorus (μg P/L) and $p_{i,d}$ = particulate inorganic phosphorus (μg P/L). Assuming that coprecipitation (a) occurs rapidly and (b) can be represented by a linear isotherm, the particulate inorganic phosphorus can be calculated as $p_{i,p} = F_p\, p_i$ where the particulate fraction is computed as

$$F_p = \frac{K_{dp}[\mathrm{CaCO_{3(s)}}]}{1 + K_{dp}[\mathrm{CaCO_{3(s)}}]} \tag{5}$$

where K_{dp} = a distribution or partition coefficient of dissolved inorganic phosphorus on calcite (M^{-1}). Note that the fraction of inorganic phosphorus in dissolved form (i.e., available) is then calculated as $F_d = 1 - F_p$. The adoption of a linear isotherm is justified because the inorganic phosphorus levels for this system are well below the levels where measured isotherms manifest any curvature (Danenlouwerse et al., 1995).

This mechanism decreases primary production in two ways: (a) it decreases phosphorus availability by sequestering a portion of the inorganic phosphorus on the calcite particles, and (b) it reduces inorganic phosphorus levels as the sorbed phosphorus is removed from the epilimnion along with the settling calcite.

Phytoplankton biomass is generated by gross primary production, which is dependent on temperature, light and inorganic phosphorus levels. The dependence of phytoplankton growth on solar radiation is formulated as an epilimnion depth-integrated, Michaelis–Menten model,

$$\phi_l = \frac{f}{k_e H} \ln\left(\frac{k_{si} + \mathrm{PAR}(0)}{k_{si} + \mathrm{PAR}(0)e^{k_e H}}\right) \tag{6}$$

where f = photoperiod (d), k_e = light extinction coefficient (/m), k_{si} = PAR half-saturation constant (μE/m^2/s), and PAR(0) = average daily photosynthetically active radiation at the lake's surface (μE/m^2/s).

A Michaelis–Menten formulation is used to represent the dependence of phytoplankton growth on dissolved inorganic phosphorus,

$$\phi_p = \frac{F_d p_i}{k_{sp} + F_d p_i} \tag{7}$$

where k_{sp} = dissolved inorganic phosphorus half-saturation constant (μg P/L).

Phytoplankton are lost by respiration/excretion, death and settling. The respiration/excretion process represents phytoplankton sinks that generate carbon dioxide, and release inorganic phosphorus. Death corresponds to phytoplankton losses that generate organic phosphorus (e.g., zooplankton grazing). The organic phosphorus pool is subject to settling and is converted to inorganic form via hydrolysis.

Secondary variables: Total phosphorus, *TP* (μg P/L), is computed as the sum of phytoplankton phosphorus, organic phosphorus and inorganic phosphorus.

$$TP = r_{pa} a_p + p_o + p_i \tag{8}$$

Gross primary production, *GPP* (mg C/m^2/d), is calculated as

$$GPP = r_{coa} \frac{V}{10^3 A_s} k_g(T) \phi_l \phi_p a_p \tag{9}$$

where r_{coa} = the phytoplankton organic carbon-to-chlorophyll a ratio (mg C/μg Chla), and A_s = the lake surface area (m^2). Net primary production, *NPP* (mg C/m^2/d), is calculated as

$$NPP = r_{coa} \frac{V}{10^3 A_s} [k_g(T) \phi_l \phi_p - k_{re}(T)] a_p \tag{10}$$

Note that the primary production rates can be integrated to generate average rates over specified time periods.

2.3.3. Inorganic chemistry sub-model

The inorganic chemistry sub-model is designed to simulate the dynamics of dissolved inorganic carbon, calcium and calcite. It also computes the individual inorganic carbon species as well as alkalinity, and specific conductance at each time step.

Dissolved inorganic carbon is taken up by photosynthesis and gained via respiration and hydrolysis. It can be also be gained or lost by carbon dioxide gas transfer, and lost or gained by calcite precipitation or dissolution, respectively.

Carbon dioxide gas transfer is driven by the CO_2 deficit and a mass-transfer coefficient computed as a function of Henry's law, temperature and wind speed. Beyond this base exchange rate, CO_2

transfer is enhanced by chemical equilibrium reactions in the water boundary layer (Emerson, 1975; Hoover and Berkshire, 1969).

$$\text{AirExchange} = Eg(T) \cdot v_{v,c}(T) \left(\frac{A_s}{V}\right) ([CO_2]_s(T) - [CO_2]) \quad (11)$$

where E_g = a chemical enhancement factor which is a function of wind speed, air temperature, water temperature and pH (Hoover and Berkshire, 1969), $v_{v,c}$ = the CO_2 air–water exchange velocity (m/d), $[CO_2]_s$ = dissolved carbon dioxide saturation concentration (M), and $[CO_2]$ = dissolved carbon dioxide concentration (M).

Due to the difficulty in characterizing the relation between wind speed and exchange velocity at low wind speeds, Schwarzenbach et al. (2003) propose a CO_2 exchange rate of 0.56 m/day for wind speeds less than 4.2 m/s. Their formula, which is also adjusted for temperature via the Schmidt Number (Sc_c), is

$$v_{v,c} = 0.56\left(\frac{Sc_c(T)}{600}\right)^{-0.67} \quad (12)$$

where Sc_c (T) is the Schmidt number for CO_2 in water as a function of temperature as computed with the following polynomial developed with a least-squares fit to data tabulated by Schwarzenbach et al. (2003)

$$Sc_c\ (T) = 1914.828 - 124.208\ T + 4.51163\,T^2 - 0.0995442\,T^3 + 0.0009934\,T^4 \quad (13)$$

Both dissolved inorganic carbon and dissolved calcium can also be removed by calcite precipitation or gained by calcite dissolution. For calcite, the reverse holds with precipitation representing a gain and dissolution a loss. In addition, calcite is subject to a settling loss.

Precipitation occurs when the ion activity product ($IAP = \gamma_2^2[Ca^{2+}][CO_3^{2-}]$) exceeds calcite's solubility product, K_{sp}. If IAP is less than K_{sp}, calcite dissolves. Both processes can be formulated as

$$\text{CalcitePrecipitation} = k_f(SA_{v,a} + SA_{v,c})(IAP - K_{sp}) \quad (14)$$

where k_f = the area-specific precipitation rate [L/(M m^2 d)], $SA_{v,a}$ = the phytoplankton volume-specific particulate surface area (m^2/L), and $SA_{v,c}$ = the calcite volume-specific particulate surface area (m^2/L). Hence, if $IAP - K_{sp}$ yields a positive value, calcite is formed. Conversely, a negative value indicates dissolution. Note that dissolution is conditional on the presence of calcite. The rate equation for calcite precipitation used here is that proposed by Inskeep and Bloom (1985) as the best fit for natural waters with high alkalinity and pH > 8. This model is consistent with the rate equations proposed by both Nancollas and Reddy (1971) and Plummer et al. (1978) for the pH and c_T levels found in Torch Lake.

Assuming spherical calcite particles, the volume-specific surface area can be formulated as a function of calcite concentration by

$$SA_{v,c} = \frac{6}{1000\rho_c d_c} r_{dc}[CaCO_{3(s)}] \quad (15)$$

where ρ_c = density of calcite crystals (=2.711 g/cm^3), d_c = diameter of calcite crystals (μm), and r_{dc} = factor to convert moles to mass of calcite (=100,000 mg $CaCO_3$/mole).

As described by Kalff (2003), picoplankton (i.e., plankton between 0.2 and 2 μm) are the dominant form of plankton in ultraoligotrophic lakes such as Torch Lake. Picoplankton have been identified as providing the primary surfaces for calcite nucleation in oligotrophic lakes (Thompson and Ferris, 1990; Hartley et al., 1995; Thompson et al., 1997; Dittrich and Obst, 2004; Dittrich et al., 2004). Dittrich et al. (2004) suggest that different picoplankton drive different mechanisms of precipitation. Some picoplankton become completely covered in calcite, die, and decay which results in calcite particles with small holes where the picoplankton had been located. Other picoplankton have calcite form on their cell walls which then peels away once the particle reaches a certain size, allowing the cells to remain viable. Since the microscopy images for Torch Lake showed no evidence of holes in the particle surfaces, the model of particle growth followed by separation is assumed to hold. Because chlorophyll a levels are relatively constant over the summer stratified period, the level of phytoplankton volume-specific particulate surface area is represented in the current model application as a constant.

The settling of calcite is a key process in the model of a lake's calcite cycle and prediction of the calcite concentration over time. The settling rate can also directly affect the rate of calcite precipitation by reducing particulate surface area for crystal growth as particles settle out of the epilimnion. The settling rate of calcite is represented by

$$\text{CalciteSettling} = v_c \cdot \left(\frac{A_t}{V}\right) \cdot [CaCO_{3(s)}] \quad (16)$$

where v_c = calcite settling velocity (m/day). The coprecipitation, or adsorption of phosphorus to calcite crystals, followed by the settling of these particles can be a significant removal mechanism of inorganic phosphorus. The inorganic phosphorus settling loss rate is computed as

$$\text{CoPrecipLoss} = v_c \cdot \left(\frac{A_t}{V}\right) \cdot F_p \cdot p_i \quad (17)$$

Secondary variables: After solving the mass balances for dissolved inorganic carbon, dissolved calcium and calcite, a chemical equilibrium model is used to compute pH along with carbon dioxide, bicarbonate and carbonate concentrations. In addition, conductivity and alkalinity are determined at each time step.

Alkalinity, *Alk* (equiv./L), is calculated as the equivalent sum of the base cations minus the conjugate bases of the strong acids (Stumm and Morgan, 1996),

$$Alk = Alk_{nc} + 2[Ca^{2+}] \quad (18)$$

where Alk_{nc} = the non-calcium alkalinity (equiv./L),

$$Alk_{nc} = 2[Mg^{2+}] + [Na^+] + [K^+] - [Cl^-] - 2[SO_4^{2-}] - [NO_3^-] \quad (19)$$

For the Torch Lake system, the non-calcium alkalinity is assumed to be constant.

Conductivity, Cond (μS/cm), can be computed from the concentrations of the major ions (APHA, 2005). First, the infinite dilution conductivity, Cond° (μS/cm), is calculated as

$$\text{Cond}^\circ = \sum_{i=1}^{n} |Z_i|\ \lambda_i\ \ \text{mM}_i \quad (20)$$

where λ_i = the equivalent conductance of the i^{th} ion (μS·cm^2/eq), Z_i = charge of the i^{th} ion, mM_i = millimolar concentration of the i^{th} ion. The specific conductance is then computed as

$$\text{Cond} = \gamma_1^2 \text{Cond}^\circ \quad (21)$$

where γ_1 = the monovalent activity coefficient.

2.3.4. Optics sub-model

The optics sub-model generates both inherent and apparent optical properties based on the output of the nutrient/phytoplankton and inorganic chemistry models.

Absorption, scattering and beam attenuation coefficients: The beam attenuation coefficient, c (m^{-1}) is calculated as (Kirk, 1983)

$$c = a + b \quad (22)$$

where a = the absorption coefficient (m^{-1}), and b = the scattering coefficient (m^{-1}). The absorption and scattering coefficients are computed as a function of the water's properties as

$$a = a_w + a_c + \alpha_{chl}\, ap + \alpha_{op}\, p_o + \alpha_i\, ISS \quad (23)$$

$$b = b_w + \beta_{chl}\, a_p + \beta_{op}\, p_o + \beta_i\, ISS + \beta_{\text{calcite}}\, 100,000\, [CaCO_{3(s)}] \quad (24)$$

where a_w = water absorption coefficient (m^{-1}), a_c = color absorption coefficient (m^{-1}), α_{chl} = phytoplankton absorption proportionality constant (m^2/mg Chla), α_{op} = organic phosphorus (i.e., detritus) absorption proportionality constant (m^2/mg P), α_i = absorption proportionality constant for inorganic suspended solids (m^2/gD), b_w = water scattering coefficient (m^{-1}), β_{chl} = phytoplankton scattering proportionality constant (m^2/mg Chla), β_{op} = scattering organic phosphorus proportionality constant (m^2/mg P), β_i = inorganic suspended solids scattering proportionality constant (m^2/gD), and β_{calcite} = calcite scattering proportionality constant (m^2/g $CaCO_3$). The factor 100,000 is included in the calcite scattering term so that β_{calcite} can be expressed in familiar mass, rather than molar, units.

Extinction coefficient: The vertical extinction coefficient is the rate of exponential attenuation of PAR with depth. It is related to model variables by (Di Toro, 1978)

$$k_e = a + (1 - \gamma)b \quad (25)$$

where γ = the fraction of particle scattering that is directly forward scattered (dimensionless).

Secchi Depth: The Secchi depth, *SD* (m), is calculated with (Tyler, 1968; Preisendorfer, 1986),

$$SD = \frac{8.69}{k_e + c} \quad (26)$$

Turbidity: Turbidity is related to scattering by (Di Toro, 1978; Kirk, 1981, 1983; Weidemann and Bannister, 1986),

$$T_N = N\, b \quad (27)$$

where *N* ranges from 0.8 to 1.27 NTU m (Effler, 1988).

2.3.5. Numerical solution

The model requires numerical solution of (1) a system of nonlinear ordinary differential equations (ODEs) representing the state-variable mass balances, and (2) a system of nonlinear algebraic equations representing the equilibrium inorganic chemistry. Algebraic manipulations are used to express the equilibrium chemistry model as a single nonlinear equation with one unknown: pH (Chapra, 1997).

Given specified initial conditions, the ODEs are integrated numerically to yield concentrations of the state variables as a function of time. For the present application this was done with a variable-step, 4th-order Runge-Kutta solver (Chapra and Canale, 2010). At each integration time step, the single nonlinear equation is solved for pH with Brent's root-location method (Chapra and Canale, 2010). The pH is then used to compute the other chemical species. In addition, all secondary variables as well as the optics sub-model are solved at the same time.

3. Results

The model was applied to simulate conditions for the epilimnion of Torch Lake from June 15 through September 15, 2006. This interval generally corresponds to the period of strong summer stratification when the pronounced decline in water clarity has been routinely observed over the past decade (Fig. 2). Although the model was specifically applied to 2006, the data set for that year was supplemented by information collected in previous years. This was useful in terms of providing a more complete understanding of calcite dynamics and was justified because the lake had not changed measurably over this period.

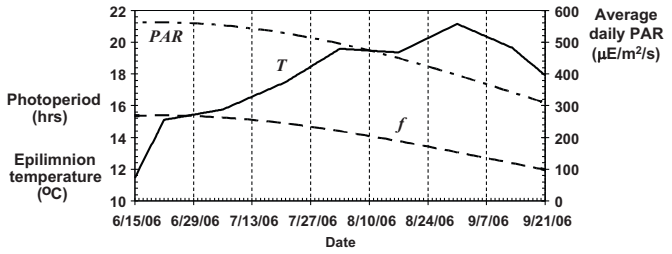

Fig. 5. Epilimnetic temperature (*T*), surface photosynthetically active radiation (PAR) and photoperiod (*f*) for Torch Lake, June to October 2006.

3.1. Forcing functions

A time series of epilimnetic water temperature was developed based on the sonde profiles. Daily photoperiods and PAR were estimated by standard calculation based on latitude, longitude, date and measured cloud cover. The calculated PAR was validated by comparison with surface Licor measurements. As shown in Fig. 5, the PAR and photoperiod decrease whereas the temperature increases over the simulation period.

3.2. Parameters

The parameters used for the model simulation are listed in Table 6. The following sections describe how these values were developed.

3.2.1. Nutrient/phytoplankton parameters

The nutrient/phytoplankton parameters are set at values that fall within the typical range used for water-quality models (e.g., Bowie et al., 1985; Jorgensen et al., 1991; Chapra, 1997). The maximum growth rate parameter was compared to published ranges. Kalff (2003) presents a regression between phytoplankton size and a saturated-light 20 °C growth rate. For 1–2 μm diameter phytoplankton, the maximum growth rate predicted is 1.8–2.0/day. Chapra (1997) gives a range of 1.5–3.0/day for phytoplankton growth rates in lakes. The phytoplankton settling velocity was set to a low value since picoplankton sinking rates are considered negligible (Kalff, 2003; Weisse, 1988).

Phosphorus coprecipitation is parameterized via the partition coefficient (K_{dp}). Values for this parameter were estimated using both sediment cores and sediment traps for Torch Lake, and compared to incorporation rates published for other lakes. Sediment cores collected in 2002 (Yohn et al., 2003) contained 0.035% phosphorus and 31.2% calcium on a dry-weight basis which yields a phosphorus-to-calcium ratio for the sediments of 1.1 mg P/g Ca. This value is potentially an overestimate of the incorporation ratio during coprecipitation due to the possible dissolution of calcium or interactions between iron and phosphorus during sedimentation.

Sediment traps were deployed during the TLA/GLEC 2005 survey at depths from 10 to 74 m over the ice-free period. The total phosphorus content of these traps ranged from 0.0185% to 0.0465% on a dry-weight basis. The sediment trap set in 2006 at a depth of 40 m was analyzed for calcium and the resulting value was 43%. Based on these values, the incorporation rate for particulate matter settling in the water column ranges from 0.4 to 1.1 mg P/g Ca.

Danenlouwerse et al. (1995) have compiled literature values for phosphorus incorporation efficiencies in calcite and corresponding dissolved inorganic phosphorus levels. This data set included two oligotrophic systems which had incorporation efficiencies of 0.4 and 0.8 mg P/g Ca for dissolved inorganic P concentrations of 1 and 5 μg P/L, respectively. In addition, they developed a Freundlich isotherm for the entire data set, which can be expressed using this

Table 6
Estimated parameter values used for Torch Lake simulation.

Parameter	Value	Units	Parameter	Value	Units
Nutrient/phytoplankton			Optics		
v_a	0.005	m d^{-1}	a_w	0.012	m^{-1}
v_o	0.05	m d^{-1}	a_c	0.05	m^{-1}
k_{de}	0.05	d^{-1}	α_{chl}	0.03	m^2 mg Chla^{-1}
k_g	1	d^{-1}	α_{op}	0.016	m^2 mg P^{-1}
k_{hy}	0.1	d^{-1}	b_w	0.0015	m^{-1}
k_{re}	0.15	d^{-1}	α_i	0	m^{-1}
k_{sp}	4	μg P L^{-1}	β_{chl}	0.1	m^2 mg Chla^{-1}
k_{si}	100	μE (m^2 s)$^{-1}$	β_{calcite}	0.6	m^2 g $CaCO_3$ $^{-1}$
K_{dp}	20,000	M^{-1}	β_{op}	0.024	m^2 mg P^{-1}
Inorganics chemistry			β_i	0.8	m^2 g D^{-1}
$v_{v,c}$ (20)	0.56	m d^{-1}	ISS	0.5	mg D L^{-1}
k_f	80,000	L (M m^2 d)$^{-1}$	γ	0.94	
v_c	1.8	m d^{-1}	N	0.8	
$SA_{v,p}$	1	cm^2 L^{-1}			

paper's nomenclature as

$$v_{pc,m} = 10.9\left(\frac{p_{i,d}}{1000}\right)^{0.5} \tag{28}$$

where $v_{pc,m}$ = incorporation efficiency of phosphorus in calcite (mg P/g Ca), and $p_{i,d}$ = dissolved inorganic phosphorus concentration (μg P/L). For the low levels of dissolved inorganic phosphorus in Torch Lake (0.5–1 μg P/L), Eq. (28) yields incorporation efficiencies of 0.24–0.49 mg P/g Ca.

Dittrich and Koschel (2002) reported a phosphorus incorporation rate of 0.72 mg P/g Ca for Lake Luzin and described the results as being well represented by Danenlouwerse et al. (1995) adsorption model. Calculations from an enclosure experiment in the Dagowsee, a stratified eutrophic hardwater lake, produced an incorporation rate of 1 mg P/g Ca (Dittrich et al., 1997).

Based on the foregoing site-specific measurements (cores and traps) and literature estimates, the average incorporation ratio for Torch Lake should be on the order of about 0.1–1 mg P/g Ca. A value of 0.5 mg P/g Ca was chosen for our model simulations. For a dissolved inorganic phosphorus concentration of 1 μg P/L, this corresponds to a distribution coefficient of 20,000 M^{-1}.

3.2.2. Inorganic chemistry parameters

Model parameters were estimated via direct measurement, literature values and calibration. The resulting values are summarized in Table 6. Details of the calibration of some of the more important parameters follow. The entire calibration is documented in Homa (2010).

3.2.2.1. Calcite precipitation rate coefficient. The precipitation rate coefficient (k_f) for the Torch Lake model was estimated by calibration of the full model. A value for k_f = 80,000 L^2/mol/m^2/day yielded the best agreement between the model predictions and the chemical (alkalinity, calcium, carbon, pH, particulate calcium) and optical data (turbidity, Secchi depth, light extinction) measurements.

All other model parameters were constrained by data measurements from Torch Lake (e.g., the settling rate by sediment trap data, etc.). The precipitation rate coefficient was not directly constrained by any data measurements, and published laboratory experiments providing calcite precipitation rates are not directly comparable to the calcite precipitation rate coefficient in the Torch Lake model. The value of k_f used in the Torch Lake model is 10–100 times smaller than published experimental rate coefficients (Homa, 2010). The primary reasons proposed for the discrepancy between the rate coefficients from lab experiments and the parameter used in Torch Lake are differences in particulate surface area and differences in mixing conditions.

The model considers particulate surface area for precipitation from both organisms (primarily picoplankton) as well as existing calcite particles. This is in line with current research on calcite precipitation on picoplankton cell surfaces as well as crystal growth. However, the laboratory experiments involved either (a) homogeneous nucleation at very high supersaturation levels, or (b) addition of calcite seed crystals, allowing for precipitation at lower saturation levels than found in natural environments. Non-calcite surfaces were not considered as nucleation sites. The rates calculated from these experimental data also involved assuming a constant particulate surface area.

Though the epilimnion of most stratified lakes can be considered 'well-mixed', it would not be surprising for the lake mixing rates to be slower than that in a stirred beaker in a laboratory experiment. Thus the fact that the published calcite precipitation rates from lab experiments are higher than the lake model rate should be considered reasonable, whereas the reverse would require additional investigation.

3.2.2.2. Calcite particle average diameter. The average particle diameter of 2 μm was calculated from a volume-weighted average of the calcite particles in the particle distribution data collected by UFI.

3.2.2.3. Phytoplankton surface area. For the Torch Lake model, the amount of fixed background surface area provided by non-calcite particles (i.e., picoplankton or other suspended particle) is set at 1 cm^2/L throughout the model time horizon. This amount is based on the surface area of non-Ca particles in the Torch Lake 2006 UFI particle distribution data. There was no evidence of a correlation between the total non-calcium particles and chlorophyll *a* for Torch Lake.

3.2.2.4. Calcite settling rate. A calcite settling velocity was calculated based on the mass of calcium, M_{Ca} (g Ca), that accumulated in the sediment traps over the summer period as in

$$v_c = \frac{M_{Ca}}{40,000 A_{trap}\ \Delta t\ [CaCO_3(s)]} \tag{29}$$

where A_{trap} = trap area (m^2), and Δt = trap deployment period (d). This resulted in a settling velocity of 1.6 m/day.

Stokes' law was used with the particle distribution data to calculate settling velocities for each particle size and a weight-averaged settling velocity was calculated by summing the fluxes for each particle size for particles with more than 50% calcium. The settling velocities calculated in this way ranged from 2.2 to 4.8 m/day. These velocities are considered an upper bound since the shape factor used in the calculations is spherical (α = 1) when clearly the par-

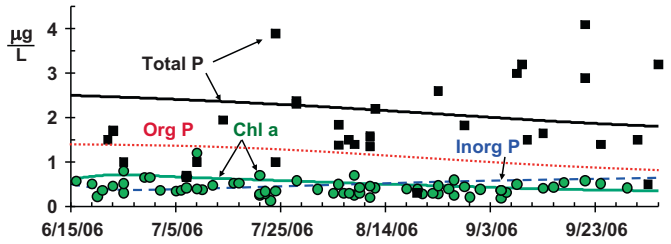

Fig. 6. Model output plotted with data for eutrophication variables: phytoplankton (solid line and circles); organic P (dotted), inorganic P (dashed) and total P (heavy solid and square points). The data represent all measurements collected from 1997 through 2006.

ticles are angular. In addition, Stokes law assumes laminar flow conditions and the actual transport regime in the Torch Lake epilimnion could in fact be turbulent at times during the summer.

The value of the settling velocity parameter used in the model is 1.8 m/day. This value was chosen by selecting a value within the range of estimates described above and matching the model estimate for particulate calcite concentration to the data. This was done after calibrating the amount of calcite precipitation based on the change in dissolved calcium, alkalinity and conductivity.

3.2.3. Optical parameters

Most of the optical parameters used in the model have been extensively studied (e.g., Kirk, 1983; Davies-Colley et al., 1993). With the exception of calcite scattering and color absorption, the values listed in Table 6 are representative of literature estimates as well as values used in other efforts to compute optical properties based on water-quality variables (e.g., Weidemann and Bannister, 1986; Effler et al., 2001; Swift et al., 2006).

Using these parameter estimates, the values for calcite scattering and color absorption were then calibrated so that the model computed values for the extinction coefficient (Eq. (25)), Secchi depth (Eq. (26)), and turbidity (Eq. (27)) matched measurements at the start of the model calculation on June 15, 2006.

3.3. Simulation results

Developing and calibrating a mass balance model of calcite precipitation creates a tool that can be used to quantify the interactions of physical, chemical and biological processes. Comparisons are shown here of model predictions against data measurements for Torch Lake from June to October 2006. The following plots demonstrate how well the Torch Lake model corresponds to observations for the optical variables and the major chemical and biological state variables. Budgets for phosphorus, calcium and carbon are also developed to quantify the relative magnitudes of the simulated processes.

3.3.1. Nutrient/phytoplankton

Fig. 6 shows model output for the nutrient/phytoplankton variables along with measured values for phytoplankton and total phosphorus concentration. Note that the 2006 measurements are supplemented with data points collected in earlier years.

As would be expected for the stable summer period, total phosphorus as well as the individual species does not vary significantly in time. The lack of strong variations is supported by the chlorophyll *a* measurements which have a long-term mean of 0.43 with a standard deviation of 0.18 µg Chla/L. Although the total phosphorus measurements exhibit more scatter (mean = 2.1 µg P/L with a standard deviation of 1.5), the lack of a strong trend is consistent with the model results. In addition, linear least squares regression was applied to the total phosphorus and chlorophyll *a* data. In both

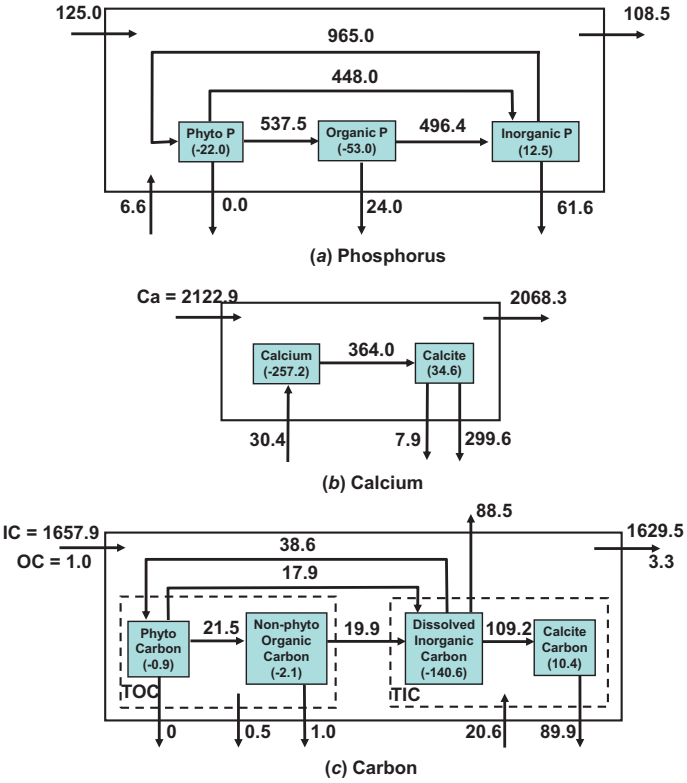

Fig. 7. Element budgets for Torch Lake epilimnion from June 15 through September 30, 2006: (a) phosphorus in µg P/m^2/d, (b) calcium in mg Ca/m^2/d, and (c) carbon in mg C/m^2/d.

cases, linear trends could not be established as both had statistically insignificant slopes (*P*-value > 5%).

Additional insight into phosphorus cycling can be developed by using the model to calculate an average budget for the simulation period. As in Fig. 7a, the results indicate that the internal cycling mechanisms (photosynthesis, respiration, death and hydrolysis) are much higher than the transport mechanisms (inflow, outflow, thermocline diffusion and settling). This is not unexpected given that we are simulating the summer period when inflows and cross-thermocline transport is diminished. Nevertheless, it is noteworthy that the loss of inorganic phosphorus due to sorption onto settling calcite particles seems to represent a significant purging mechanism for this lake.

3.3.2. Inorganic chemistry

Model output along with direct measurements for dissolved calcium and the calculated variables, alkalinity, specific conductance and pH, are shown in Fig. 8. Due primarily to calcite precipitation, the data and simulation results for calcium, alkalinity and specific conductance show a consistent decline over the entire simulation period (Fig. 8a–c). The dissolved calcium concentration decreases as calcium moves from the dissolved to the solid phase due to calcite precipitation. Alkalinity also decreases as calcite precipitation removes carbonate. Conductivity decreases due to the removal of both CO_3^{2-} and Ca^{2+} since each ion contributes to the specific conductance.

The change in pH is due to many simultaneous processes acting on inorganic carbon and alkalinity. The loss of CO_2 to the air and primary production should raise pH but the loss of CO_3^{2-} to calcite precipitation dominates through August and leads to the decline in pH. As the calcite precipitation declines at the end of August, air exchange of CO_2 continues and the pH starts to rise in September.

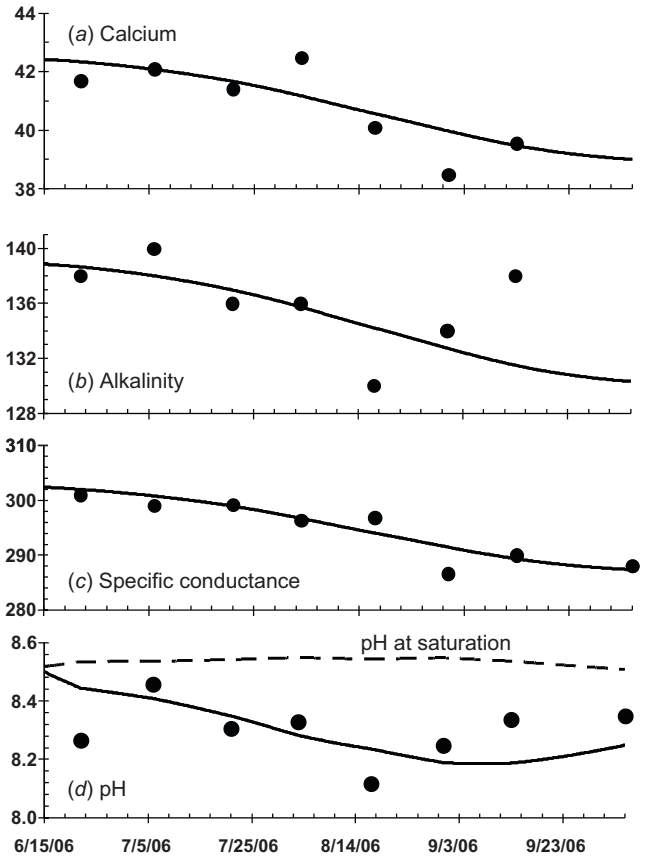

Fig. 8. Model output plotted with data for inorganic chemistry variables: (a) calcium, (b) alkalinity, (c) specific conductance, and (d) pH. The dashed line in (d) is the pH at CO_2 saturation.

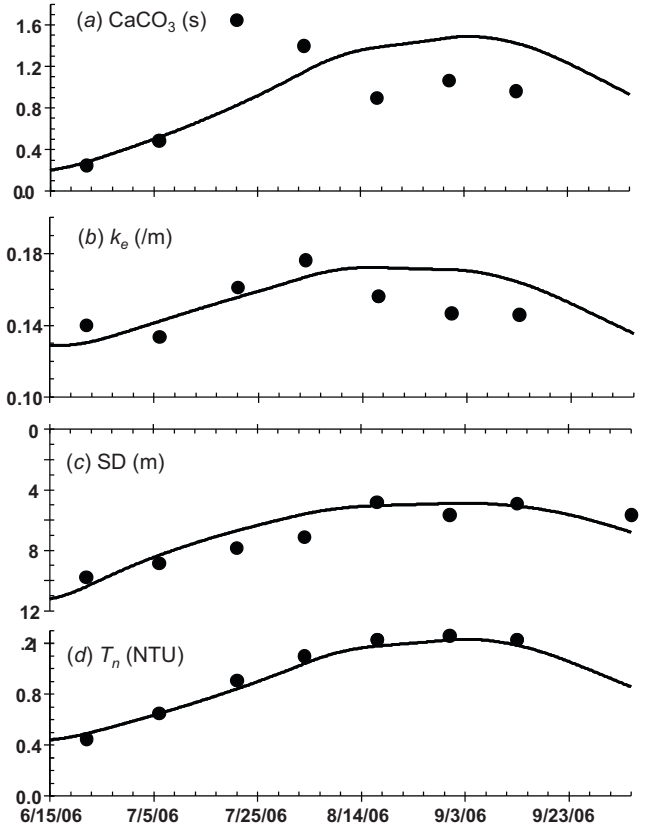

Fig. 9. Model output plotted against data for (a) calcite state variable [$CaCO_{3(s)}$] and optics calculated variables: (b) light extinction (k_e), (c) Secchi depth (SD) and (d) turbidity (T_N).

In addition to the time-series comparisons, the model is used to calculate an average calcium budget for the simulation period in Fig. 7b. While the inflow and outflow are high (due primarily to the high concentrations of dissolved calcium), the net flow (inflow – outflow = 54.6 mg Ca/m^2/d) is small relative to the calcite precipitation and settling fluxes. For example, the magnitude of precipitation and settling losses are on the order of 6 times higher and result in a net total calcium loss for the epilimnion during the summer stratified period.

The modeled precipitation rate over time averaged 0.11 mg/L/day. Ranges of precipitation rates reported for other lakes are 0.2 ± 0.1 mg/L/day (Ramisch et al., 1999; Holzbecher and Nutzmann, 2000). The modeled value is thus consistent with rates published for other lakes.

3.3.3. Optics

The model output for the major variables that influence (i.e., calcite) and quantify (i.e., extinction coefficient, Secchi depth and turbidity) the lake's optical quality are shown along with data in Fig. 9. As displayed in Fig. 9a, the calcite rises significantly between June 15 and the beginning of August. The precipitation rate then slows down until a peak is reached in early September. Thereafter, decreasing temperatures reduce precipitation to the point that settling dominates calcite dynamics and levels decline.

As illustrated in Fig. 9b–d, this temporal evolution of calcite concentration then impacts epilimnion optics. Of the three optical variables, light extinction is more dominated by absorption (which for calcite is zero); though scattering does also contribute [Eq. (25)]. Hence the effect on extinction, though evident in both the data and calculated values, is moderate. The model for Secchi depth in Eq. (26) is also a function of both absorption and scattering with the latter being more important. Consequently, the impact of calcite scattering on Secchi depth is more pronounced. Because turbidity is directly proportional to scattering [Eq. (27)], the simulated turbidity closely follows the calcite trend.

3.3.4. Carbon budget

The model can be used to quantify budgets for both organic and inorganic carbon. As in Fig. 7c, inflow and outflow of total inorganic carbon, which is overwhelmingly bicarbonate ion, dwarf the other mass transfers. However, just as was the case for calcium, the net flow is relatively small.

Of the other input–output mechanisms, the two most important carbon losses are both inorganic. These are an atmospheric efflux of carbon dioxide and the precipitation and settling loss of calcite. Interestingly, these carbon fluxes have opposite effects on pH, with loss of carbon dioxide, raising pH, and loss of carbonate,

Table 7
Estimates of summer primary production in mg C/m^2/d for Torch Lake.

Source	Primary production rate	Source
Regression (general)	6–8	Kalff (2003)
Regression (Great Lakes)	80	Chapra and Dobson (1981)
50% of Lake Superior rate	70	Chapra and Dobson (1981)
Regression (Great Lakes)	55	Vollenweider et al. (1974)
Char Lake	11	Dodson (2004)
Lake 239	55	Dodson (2004)
Model		
Gross	38.6	
Net	20.7	

lowering pH. As might be expected for an ultraoligotrophic system dominated by picoplankton, organic input-output fluxes are minimal.

The largest internal transfer is the conversion of dissolved inorganic carbon (i.e., carbonate) to calcite via precipitation. About 78% of this calcite production is ultimately lost from the epilimnion via settling.

The model estimate of inorganic carbon uptake by phytoplankton is consistent with levels of primary production for ultraoligotrophic systems (Table 7). Given the average measured values of *TP* (2.5 μg/L) and chlorophyll *a* (0.5 μg/L), Torch Lake is clearly ultraoligotrophic. Various regression equations (Vollenweider et al., 1974; Chapra and Dobson, 1981; Kalff, 2003) allow estimates of primary production given an average chlorophyll *a* concentration. These equations predict a range for *NPP* of 20–80 mg C/m^2/day given Torch Lake's average chlorophyll *a* level. Note that two of the three regressions are based on data from the Great Lakes but given the proximity and similarity in chemistry, the Great Lakes should be a reasonable estimator of reasonable ranges for Torch Lake primary production. However, the data used for the Great Lakes regressions likely includes spring blooms so they should be considered upper limits for bounding estimates of Torch summer primary production levels.

In addition to regression equations, a sense of reasonable predictions for Torch Lake are provided by direct comparisons with other lakes with similar *TP* and chlorophyll *a* levels (although it should be noted that few north temperate lakes have *TP* and chlorophyll *a* levels as low as Torch Lake). From values compiled by Dodson (2004), Torch Lake should fall between Char Lake (*NPP* = 4.1 mg C/m^2/d) and Lake 239 (*NPP* = 58.4 mg C/m^2/day). Of the Great Lakes, Lake Superior's trophic state is the closest, with *TP* of 4.6 μg/L, chlorophyll *a* of 0.7 μg/L and *NPP* of 137 mg C/m^2/day (Chapra and Dobson, 1981). These estimates represent lake-wide averages for the ice-free period (Vollenweider et al., 1974). Note that Torch Lake's *TP* averages half that of Lake Superior and has a lower chlorophyll *a*, so we could expect that it would have a lower *NPP*.

These literature values were used to estimate possible ranges of primary production in Torch Lake. For lakes in a north-temperate climate where ice-free period rates were reported (Vollenweider et al., 1974) it was assumed that the winter rate was 50% of the ice-free rate, and both rates were reported as bounds.

Torch Lake primary production may be significantly lower than the estimates based on the Great Lakes because the Great Lakes data include spring phytoplankton blooms, whereas there is no such bloom in the summer in Torch Lake. There is also much uncertainty in the estimate from the Kalff (2003) regression since the output is "Volumetric Photosynthesis in mgO_2/m^3/hr" and thus required conversion to both an areal and a daily rate, and may better represent gross, and not net, primary production. However, despite the uncertainty, the rate was still included here for comparison. It was considered to be a daylight rate and thus converted to a daily rate using a 12-h photoperiod.

4. Analysis

The factors affecting the rate of calcite precipitation include temperature, air exchange, photosynthesis, respiration, and decomposition. The direct effects of temperature on the precipitation rate take place through chemical equilibrium reactions that are modeled as occurring instantly, or in other words as a "local equilibrium." The indirect effects of temperature on the precipitation rate occur through the biological processes of photosynthesis and respiration/decomposition, and the air–water exchange of carbon dioxide. These processes affect the precipitation rate through the removal or addition of carbon dioxide which shifts the carbonate equilibrium (adding/removing c_T and decreasing/increasing pH), potentially changing the CO_3^{2-} concentration in the water and thus the degree of calcium carbonate saturation. In addition, phytoplankton drives the precipitation rate by providing particulate surface area for the growth of calcite.

Table 8
Summary of the main and interaction effects of various factors on average calcite precipitation rate (mg C/m^2/d) for the surface layer of Torch Lake in summer.

Factors	Effect
Calibration	109.2
Average	55.1
Main effects	
Temp	49.8
Air	35.5
PrPr	1.1
Interactions	
Temp–Air	22.4
Temp–PrPr	0.0
Air–PrPr	−0.3
Temp–Air–PrPr	−0.2

The model was used to evaluate which mechanisms drive calcite precipitation in Torch Lake. To do this, we employ a factorial experimental design methodology to quantify the relative impact of the various factors driving precipitation (Box et al., 2005; Berthouex and Brown, 1994). Though this approach is most commonly employed for experimental design (i.e., to reduce cost by running fewer data-collection experiments), the benefit of using it here despite minimal cost per experiment (model run) is the insight it provides into the interaction effects of the different factors influencing calcite precipitation.

In order to apply a factorial design, each model run is viewed as an "experiment" yielding a single response variable. For the present application, the average calcite precipitation rate over the simulation period is a suitable response variable. We will express the precipitation rate in units of mg C/m^2/d so that the results are consistent with the carbon budget previously developed in Fig. 7c.

The analysis then requires the specification of a number of factors that have an effect on the response variable along with lower and upper levels for these factors. In our case, we will examine three factors: temperature (Temp), air–water exchange of carbon dioxide (Air), and biological and chemical processes such as primary production that involve the uptake and release of carbon dioxide (PrPr). The lower and upper levels for these factors are defined as:

- Temp. The lower level involves having no temperature rise over the simulation period. That is, the epilimnion is held at its initial value at the start of the computation (10°C). The upper level is defined as the typical temperature rise (from 10 °C to 22 °C) that occurs over the summer.
- Air. The lower level is defined as zero air–water gas transfer whereas the upper level corresponds to the calibrated model.
- PrPr. The lower level corresponds to setting all biochemical processes to zero. These include photosynthesis, respiration, and death. In addition, because we are using organic phosphorus as a surrogate for organic carbon, hydrolysis is set to zero. The upper level corresponds to the calibrated model.

Table 8 shows the results of the analysis. The average calcite precipitation rate for the baseline calibration simulation (temperature normal and both air exchange and primary production processes included) is 109.2 mg C/m^2/d. The average value of 55.1 mg C/m^2/d is the average of all 8 model runs (2^3) and is lower than the calibration base run because it includes the scenarios when the temperature is fixed at 10 °C and there is no air exchange or primary production all of which lead to lower precipitation rates.

The next three rows in Table 8 show the direct effect of each individual factor on the precipitation rate. These numbers are the difference between two averages – the average of all the runs with the parameter low and the average of all the runs with the parameter high. The values indicate that both temperature and air–water exchange have a strong influence on precipitation in this lake. The magnitudes also suggest that keeping temperature fixed at 10 °C (i.e., it does not gradually increase through the summer) has a somewhat greater impact on precipitation (a decrease of 49.8 mg C/m^2/d) than not allowing air exchange of CO_2 (a decrease of 35.5 mg C/m^2/d) In contrast, the effect of the biological processes is much less pronounced with only 1.1 mg C/m^2/d.

The final four rows of Table 8 quantify the interactions among the processes; that is, the effect of a factor being influenced by the setting of another factor (Berthouex and Brown, 1994). The high value for the Temp–Air interaction (22.4 mg C/m^2/d) underscores the point that the individual effects of these two mechanisms cannot be simply added together to create their combined effect.

In comparison, the results show that the presence or absence of primary production has a negligible effect. Note that this effect is limited to the change in pH driving calcite saturation levels caused by photosynthesis and respiration/decomposition processes. Other possible roles of picoplankton in changing conditions in their microenvironment that facilitate calcite precipitation are undoubtedly important, but are beyond the scope of the current study.

5. Discussion

The evolution and impact of calcite in lake systems involves the interplay of various physical, chemical and biological processes. Although direct measurements are useful for quantifying individual processes, a mass-balance model provides a holistic framework for integrating such processes and understanding their collective impact.

However, as has been well-documented, such models must strike a balance between model reliability and complexity (Chapra, 2003). In particular, frameworks should be sufficiently comprehensive to encompass key mechanisms and interactions while being sufficiently simple so that model parameters can be adequately identified (e.g., Reichert and Omlin, 1997; Omlin et al., 2001b; Arhonditsis and Brett, 2004; Reichert and Borsuk, 2005).

In the case of calcite, we have attempted to strike this balance. In order to be comprehensive, we have coupled nutrient/phytoplankton, chemical equilibria and optics models into a single, unified framework. Such coupling is not typically employed (or even necessary) for simulating many aspects of lake water quality. For example, outside of frameworks specifically designed to simulated problems such as acid rain, most state-of-the-art lake models (e.g., Hamilton and Schladow, 1997; Omlin et al., 2001a; Arhonditsis and Brett, 2005) do not explicitly compute pH and other aspects of equilibrium inorganic chemistry. Further, aside from a few exemplary cases (e.g., Swift et al., 2006; Effler et al., 2008), lake optics are usually modeled in a cursory fashion. For example, the effect of particles (other than chlorophyll) on light scattering and absorption is not typically modeled and inherent and apparent optical properties (such as Secchi depth and turbidity) are not calculated.

Beyond allowing us to adequately address the calcite problem, the model's broader scope has the ancillary benefit of providing additional estimates of common measurements for model calibration. Thus, we can employ secondary variables such as specific conductance, pH and turbidity to assess model performance.

At the same time that we have tried to be sufficiently comprehensive, we have also tried to be parsimonious. By employing simple models and limiting the analysis to the epilimnion during summer stratification, we have endeavored to define a minimum number of parameters that are consistent with the available data for this system. As previously stated, such a parsimonious approach reduces uncertainty by using all the available data (including both time series and process measurements such as sediment traps) to calibrate the fewest number of parameters. For the case of Torch Lake the results indicate that the biological processes have a minimal effect on calcite precipitation and thus on the change in transparency. The nutrient/phytoplankton sub model was still included here both to allow the sensitivity analysis on the Torch Lake model and to allow the model to be applied to further studies of more productive lakes.

The results indicate that physicochemical processes govern the dramatic and persistent decrease in transparency that occurs each summer in this lake. In particular, the combined effect of rising temperature and carbon dioxide gas transfer lead to sufficient calcite generation to induce the substantial and chronic decrease in observed water clarity.

Looking at the original question of whether the seasonal temperature change or primary production was the driver of calcite precipitation in Torch Lake, we see from our factorial analyses that temperature is a much more significant factor in driving precipitation. But there is some complexity behind this basic conclusion. In particular, the effect of decreased solubility, which is often cited as the main temperature effect, is small compared to other temperature effects. For example, a much more significant temperature effect is the resulting decrease in CO_2 solubility and thus increased oversaturation resulting in CO_2 loss to the air.

Although the model has been developed as a descriptive, data synthesis tool, there is clearly a need for predictive management models to address the calcite problem in hardwater lakes. Aside from Torch Lake, some of the most beautiful and highly valued lakes in the world have sufficient levels of calcium that they are vulnerable to whitings. These include important lakes in North America (e.g., Lake Michigan and many of the Finger Lakes) and Europe (e.g., Lake Geneva, Lac d'Annecy and Lake Constance). Thus, we hope that our work represents a positive step towards the development of a management tool for such systems.

In order to do this, however, additional research is necessary. An opportunity for further study lies in applying the calcite precipitation model to other lakes, particularly to higher productivity systems. This will allow testing and perhaps modifying the model approach in order to develop a more robust and generally applicable model of calcite precipitation.

The model performed well at describing available data for calcite precipitation in summer given processes in the lake's epilimnion. Additional data collection may allow a more refined model to provide insights into different questions such as the role of the sediments over annual cycles or the calcite levels in the colder seasons. The model could be expanded in time and space. This includes modeling a full annual cycle and even extending the time horizon to include multiple years. The one layer model could be extended to be a multi-layer model with the addition of the hypolimnion and possibly the thermocline, as well as the lake sediments. The latter is particularly important as it would be critical to capturing the magnitude of permanent calcium losses to the sediments.

In addition to these extensions, there are further opportunities to improve the capabilities of the precipitation model by adding detail. Modeling the calcite particle size as dynamic would allow inclusion of the effects of particle size on light scattering as well as availability of surface area for calcite growth and variable settling rates.

Finally, from the standpoint of management applications, a critical area of research would be the explicit simulation of picoplankton population dynamics. Most current state-of-

the-art eutrophication-oriented, water-quality (i.e., management-oriented) models allow 3 or 4 functional groups of phytoplankton (e.g., Hamilton and Schladow, 1997; Omlin et al., 2001a; Arhonditsis and Brett, 2005). Although efforts have been made to simulate picoplankton dynamics within research contexts (e.g., Kumar et al., 1991; Fasham et al., 1999), such constructs have yet to be incorporated into water-quality models. Because they play such a large role as nucleation sites, modeling seasonal levels of picoplankton should be a critically important first step to developing a truly predictive framework for simulating calcite crystal formation in lakes.

6. Conclusions

In conclusion, the model developed in this paper provides a representation of calcite precipitation driven by physical, chemical and biological processes, and demonstrates that it is possible for the change in water clarity to be explained by calcite using standard optical models. The analyses provided here show that temperature affects the rate of calcite precipitation in many ways. The direct effects include reducing the solubility, represented by the temperature dependence of K_{sp}, the shift in the carbon system represented by temperature dependence of K_1 and K_2, as well as the increase in the chemical reaction rates represented by the Arrhenius effect. Temperature also affects the rate of calcite precipitation indirectly through the temperature dependences of primary production rates, the air exchange rate and the timing and length of the stratified period in a lake. As we have demonstrated, air exchange is a critical component that needs to be considered when analyzing the drivers of calcite precipitation in oligotrophic lakes. Mass balance models can be useful tools in furthering our understanding of the various processes involved in calcite precipitation in lakes.

Acknowledgements

Thanks to Dean Branson, Norton Bretz and the rest of the field team at the Three Lakes Association. Helpful suggestions and guidance were provided by Linfield Brown, Marianne Moore, and Marc Edwards. Measurement and guidance on lake optics were contributed by Steven Effler and Feng Peng of the Upstate Freshwater Institute.

References

Allison, J.D., Brown, D.S., Novo-Gradac, K.J. 1991. MINTEQA2/PRODEFA2, a geochemical assessment model for environmental systems: Version 3.0 User's manual. U.S. EPA, ORD, Athens, GA, EPA/600/3-91/021.

APHA, 2005. Standard Methods for the Examination of Water and Wastewater, 21st ed. American Public Health Association, American Water Works Association and Water Environment Federation, Washington, DC.

Arhonditsis, G.B., Brett, M.T., 2004. Evaluation of the current state of mechanistic aquatic biogeochemical modeling. Where are we? Marine Ecology Progress Series 271, 13–26.

Arhonditsis, G.B., Brett, M.T., 2005. Eutrophication model for Lake Washington (USA) Part I. Model description and sensitivity analysis. Ecol. Model. 187 (2–3), 140–178.

Berthouex, P.M., Brown, L.C. (1994). Statistics for Environmental Engineers, Vol. 335 Lewis Publishers, Boca Raton, FL.

Bowie, G.L., Mills, W.B., Porcella, D.B., Campbell, C.L., Pagenkopf, J.R., Rupp, G.L., Johnson, K.M., Chan, P.W.H., Gherini, S.A., Chamberlin, C.E., 1985. Rates, constants, and kinetic formulations in surface water quality modeling. U.S. EPA, ORD, Athens, GA, ERL, EPA/600/3-85/040.

Box, G.E., Hunter, W.G., Hunter, J.S., 2005. Statistics for Experimenters: Design, Innovation, and Discovery, 2nd ed. Wiley, New York.

Bretz, N., Branson, D., Hannert, T., Roush, P., Endicott, D., 2005. Characterization of Groundwater Phosphorus in Torch Lake. Three Lakes Association, Bellaire, MI.

Canale, R., DePalma, L., Vogel, A., 1975. A food web model for Lake Michigan, Part 2-model formulation and preliminary verification. University of Michigan Sea Grant, Technical Report No. 43, Ann Arbor, MI.

Carlson, R.E., 1977. A trophic state index for lakes. Limnol. Oceanogr. 22, 361–369.

Chapra, S.C., 1979. Applying phosphorus loading models to embayments. Limnol. Oceanogr. 24, 163–168.

Chapra, S.C., 1997. Surface Water Quality Modeling. McGraw-Hill, New York.

Chapra, S.C., 2003. Engineering Water Quality Models and TMDLs. J. Water Resour. Plan. Manage. 129 (4), 247–256.

Chapra, S.C., Canale, R.P., 2010. Numerical Methods for Engineers, 6th ed. McGraw-Hill, New York.

Chapra, S.C., Dobson, H.F.H., 1981. Quantification of the lake trophic typologies of Naumann (surface quality) and Thienemann (oxygen) with special reference to the Great Lakes. Int. Assoc. Great Lakes Res. 7 (2), 182–193.

Danenlouwerse, H.J., Lijklema, L., Coenraats, M., 1995. Coprecipitation of phosphate with calcium-carbonate in Lake Veluwe. Water Res. 29 (7), 1781–1785.

Davies, C.W., 1962. Ion Association. Elsevier Press, Amsterdam, The Netherlands.

Davies-Colley, R.J., Vant, W.N., Smith, D.G., 1993. Colour and Clarity of Natural Waters: Science and Management of Optical Water Quality. Ellis-Horwood, New York.

Di Toro, D.M., 1978. Optics of turbid estuarine waters: approximations and Applications. Water Res. 12, 1059–1068.

Dittrich, M., Koschel, R., 2002. Interactions between calcite precipitation (natural and artificial) and phosphorus cycle in the hardwater lake. Hydrobiologia 469, 49–57.

Dittrich, M., Obst, M., 2004. Are picoplankton responsible for calcite precipitation in lakes? Ambio 33 (8), 559–564.

Dittrich, M., Dittrich, T., Sieber, I., Koschel, R., 1997. A balance analysis of phosphorus elimination by artificial calcite precipitation in a stratified hardwater lake. Water Res. 31 (2), 237–248.

Dittrich, M., Kurz, P., Wehrli, B., 2004. The role of autotrophic picocyanobacteria in calcite precipitation in an oligotrophic lake. Geomicrobiol. J. 21 (1), 45–53.

Dodson, S.I., 2004. Introduction to Limnology. McGraw-Hill, New York.

Effler, S.W., 1988. Secchi disc transparency and turbidity. J. Environ. Eng. 114 (6), 1436–1447.

Effler, S.W., Gelda, R.K., Bloomfield, J.A., Quinn, S.O., Johnson, D.L., 2001. Modeling the effects of tripton on water clarity: Lake Champlain. J. Water Resour. Plan. Manage. 127 (4), 224–234.

Effler, S.W., Gelda, R.K., Perkins, M.G., Peng, F., Hairston, N.G., Kearns, C.M., 2008. Patterns and modeling of the long-term optics record of Onondaga Lake, New York. Fundam. Appl. Limnol. 172 (3), 217–237.

Emerson, S., 1975. Chemically enhanced CO_2 gas exchange in a eutrophic lake: a general model. Limnol. Oceanogr. 20 (5), 743–753.

Endicott, D., Branson, D., Bretz, N., Hannert, T, March 17, 2006, "Development of a predictive nutrient-based water quality model for Torch Lake", Three Lakes Association, Bellaire, Michigan 49615, MDEQ Grant PO# 761P40021.

Fasham, M.J.R., Boyd, P.W., Savidge, G., 1999. Modeling the relative contributions of autotrophs and heterotrophs to carbon flow at a Lagrangian JGOFS station in the Northeast Atlantic: the importance of DOC. Limnol. Oceanogr. 44 (1), 80–94.

Hamilton, D., Schladow, S., 1997. Prediction of water quality in lakes and reservoirs. Part 1: Model description. Ecol. Model. 96 (1–3), 91–110.

Hartley, A.M., House, W.A., Callow, M.E., Leadbeater, B.S.C., 1995. The role of a green-alga in the precipitation of calcite and the coprecipitation of phosphate in freshwater. Int. Rev. Gesamt. Hydrobiol. 80 (3), 385–401.

Hodell, D.A., Schelske, C.L., Fahnenstiel, G.L., Robbins, L.L., 1998. Biologically induced calcite and its isotopic composition in Lake Ontario. Limnol. Oceanogr. 43 (2), 187–199.

Holzbecher, E, Nutzmann, G., 2000. Influence of the subsurface watershed on eutrophication—Lake Stechlin case study. Ecol. Eng. 16 (1), 31–38.

Homa, E.S., 2010. "Mass balance modeling of calcite in the epilimnion of an ultra-oligotrophic lake" thesis, presented to Tufts University, Medford, MA, in partial fulfillment of the requirements for the degree of Doctor of Philosophy.

Hoover, T.E., Berkshire, D.C., 1969. Effects of hydration on carbon dioxide exchange rates across an air–water interface. J. Geophys. Res. 92, 1937–1949.

House, W.A., 1990. The prediction of phosphate coprecipitation with calcite in freshwaters. Water Res. 24 (8), 1017–1023.

Inskeep, W.P, Bloom, P.R., 1985. An evaluation of rate equations for calcite precipitation kinetics at pCO_2 less than 0.01 atm and pH greater than 8. Geochim. Cosmochim. Acta 49 (10), 2165–2180.

Jorgensen, S.E., Nielsen, S.N., Jorgensen, L.A., 1991. Handbook of Ecological Parameters and Ecotoxicology. Pergamon Press, Amsterdam.

Kalff, J., 2003. Limnology. Prentice-Hall, Englewood Cliffs, NJ.

Kirk, J.T.O., 1981. Estimation of the scattering coefficient of natural waters using underwater irradiance measurements. Aust. J. Mar. Freshwater Res. 32 (3), 533–539.

Kirk, J.T.O., 1983. Light and Photosynthesis in Aquatic Ecosystems. Cambridge Univ. Press, New York, NY.

Kleiner, J., 1988. Coprecipitation of phosphate with calcite in lake water—a laboratory experiment modeling phosphorus removal with calcite in Lake Constance. Water Res. 22 (10), 1259–1265.

Kumar, S.K., Vincent, W.F., Austin, P.C., Wake, G.C., 1991. Picoplankton and marine food chain dynamics in a variable mixed-layer: a reaction–diffusion model. Ecol. Model. 57 (3–4), 193–219.

Morel, F., Hering, J.G., 1993. Principles and Applications of Aquatic Chemistry. Wiley-Interscience, New York.

Nancollas, G.H., Reddy, M.M., 1971. Crystallization of calcium carbonate. 2. Calcite growth mechanism. J. Colloid Interface Sci. 37 (4), 824-&.

Omlin, M., Reichert, P., Forster, R., 2001a. Biogeochemical model of Lake Zürich: model equations and results. Ecol. Model. 141 (1–3), 77–103.

Omlin, M., Brun, R., Reichert, P., 2001b. Biogeochemical model of Lake Zürich: sensitivity, identifiability and uncertainty analysis. Ecol. Model. 141 (1–3), 105–123.

Peng, F., Effler, S.W., 2005. Inorganic tripton in the Finger Lakes of New York: importance to optical characteristics. Hydrobiologia 543, 259–277.
Plummer, L.N., Wigley, T.M.L., Parkhurst, D.L., 1978. Kinetics of calcite dissolution in CO_2-water systems at 5-degrees-C to 60-degrees-C and 0.0 to 1.0 atm CO_2. Am. J. Sci. 278 (2), 179–216.
Plummer, L.N., Busenberg, E., 1982. The solubilities of calcite, aragonite and vaterite in CO_2–H_2O solutions between 0 and 90 °C, and an evaluation of the aqueous model for the system $CaCO_3$–CO_2–H_2O. Geochim. Cosmochim. 46, 1011–1040.
Preisendorfer, R.W., 1986. Secchi disc science: visual optics of natural waters. Limnol. Oceanogr. 31 (5), 909–926.
Ramisch, F., Dittrich, M., Mattenberger, C., Wehrli, B., Wueest, A., 1999. Calcite dissolution in two deep eutrophic lakes. Geochim. Cosmochim. Acta. 63, 3349–3356, doi:10.1016/S0016-7037(99)00256-2.
Redfield, A.C., Ketchum, B.H., Richards, F.A., 1963. The influence of organisms on the composition of seawater. In: Hill, M.N. (Ed.), The Sea, Vol. 2. Wiley-Interscience, NY, pp. 27–46.
Reichert, P., Omlin, M., 1997. On the usefulness of overparameterized ecological models. Ecol. Model. 95 (1997), 289–299.
Reynolds, C.S., 1984. The Ecology of Freshwater Phytoplankton. Cambridge University Press, Cambridge, UK.
Schnoor, J.L., O'Connor, D.J., 1980. A steady state eutrophication model for lakes. Water Res. 14 (11), 1651–1665.
Schwarzenbach, R.P., Gschwend, P.M., Imboden, D.M., 2003. Environmental Organic Chemistry. Wiley-Interscience, NY.
Stumm, W., Morgan, J.J., 1996. Aquatic Chemistry, 3rd ed. Wiley-Interscience, New York, 1022 pp.
Swift, T.J., Perez-Losada, J., Schladow, S.G., Reuter, J.E., Jassby, A.D., Goldman, C.R., 2006. Water clarity modeling in Lake Tahoe: linking suspended matter characteristics to Secchi depth. Aquat. Sci. 68, 1–15.
Thompson, J.B., Ferris, F.G., 1990. Cyanobacterial precipitation of gypsum, calcite, and magnesite from natural alkaline lake water. Geology 18 (10), 995–998.
Thompson, J.B., SchultzeLam, S., Beveridge, T.J., DesMarais, D.J., 1997. Whiting events: biogenic origin due to the photosynthetic activity of cyanobacterial picoplankton. Limnol. Oceanogr. 42 (1), 133–141.
Tyler, J.E., 1968. Secchi disc. Limnol. Oceanogr. 13 (1), 1–6.
Vollenweider, R., Munawar, M., Stadelmann, P., 1974. Comparative review of phytoplankton and primary production in Laurentian Great Lakes. J. Fish. Res. Board Canada 31 (5), 739–762.
Weidemann, A.D., Bannister, T.T., 1986. Absorption and scattering coefficients in Irondequoit Bay. Limnol. Oceanogr. 31, 567–583.
Weisse, T., 1988. Dynamics of autotrophic picoplankton in Lake Constance. J. Plankton Res. 10 (6), 1179–1188.
Wetzel, R.G., 1983. Limnology. Saunders, Philadelphia, PA.
Yohn, S.S., Parsons, M.J., Long, D.T., Giesy, J.P., Scholle, L.K., Patino, L.C., 2003. Inland Lakes Sediment Trends: Sediment Analysis Results for Six Michigan Lakes, Yearly Report 2002–2003. Michigan Department of Environmental Quality, East Lansing, MI.